RUSSIAN JOURNAL *of* EARTH SCIENCES

RESULTS OF NUMERICAL MODELLING OF THE PROBLEM OF VIDEO PULSE GROUND PENETRATING RADAR RESEARCH IN FRESHWATER BODIES

O. A. Gulevich*,1, L. B. Volkomirskaya1, I. V. Mingalev2, V. V. Varenkov1,
Z. V. Suvorova2, O. I. Akhmetov2, O. V. Mingalev2, and A. E. Reznikov1

1*Pushkov Institute of Terrestrial Magnetism, Ionosphere and Radio Wave Propagation, Russian Academy of Sciences (IZMIRAN), Troitsk, Moscow, Russia*
2*Polar Geophysical Institute, Apatity, Russia*

Ground-penetrating radar profiling on the surface of water bodies is applied in various geological and engineering studies. Here, we present the results of numerical simulation of the propagation of a video pulse electromagnetic signal in a freshwater body with gradients of the permittivity and electrical conductivity in the near-bottom layer. The method of numerical solutions of Maxwell's equations in the time domain is applied, in the setting for rapidly changing processes, without restrictions on the magnitude of the change in the parameters of the medium. The results make it possible to explain the apparent decrease in water depth according to GPR data in comparison with the true depth and the appearance of additional reflecting boundaries on radargrams in the bottom layer.

Keywords: GPR, numerical modelling, video pulse, water depth.

1 INTRODUCTION

Freshwater bodies are resistive and can therefore be penetrated by ground-penetrating radar (GPR) where radar can be used for sub-bottom profiling, to investigate water depth and the thickness and extent of sediments [*Bristow and Jol*, 2003]. Lake deltas have been studied by Jol and Smith [*Jol and Smith*, 1991; *Smith and Jol*, 1992]. In [*Bobrov et al.*, 2008], a thorough GPR study depicted the halocline – a strong salinity gradient between water layers at the mouth of a river flowing into the sea.

Estimates of water depth are fundamental for most studies of water bodies and based on recalculating the time delays of the registered GPR signals using the permittivity value $\varepsilon = 81$. Nevertheless, some loss of accuracy may occur, not only due to the dependence of permittivity on water mineralization and temperature [*Owen et al.*, 1961; *Archer and Wang*, 1990; *Somaraju and Trumpf*, 2006; *Catenaccio et al.*, 2003] but also due to inhomogeneities in the near-bottom layer, which usually accumulate plant material, mud and silt in the natural environment.

In this paper, we consider the results of numerical simulation of the propagation of a wideband video pulse signal in a water body model with a near-bottom gradient layer. For the theoretical description of video impulse impact on real media, the approximation of small absorption and a slow change in the source parameters is not fulfilled, imposing restrictions on the use of commonly used separable solutions of Maxwell's equations [*Schwarzburg*, 1998; *Gulevich*, 2020]. We consider the interaction of a video pulse with a real medium based on numerical solutions of Maxwell's equations in the time domain, in a general setting for rapidly changing processes, without restrictions on the magnitude of the change in the parameters of the medium.

Apparently, the most popular method for the numerical integration of Maxwell's equations in the time domain is the Finite-Difference Time-Domain method (FDTD) [*Kane*, 1966; *Paul and Railton*, 2012; *Simpson and Taflove*, 2007; *Simpson*, 2009; *Yu and Simpson*, 2010]. This method became the basis for the development of numerical modelling in GPR, where the FDTD method was implemented in the open source gprMax software [*Giannopoulos*, 2005; *Warren et al.*, 2016].

*Corresponding author: o.a.gulevich@gmail.com

However, in the FDTD method, there is a limitation on the integration step in time, associated with the conductivity of the medium, and it consists in the fact that, in order to achieve acceptable accuracy, the integration step is required to be small in comparison with the time of field change due to the conductivity of the medium. On the other hand, a too-small time step in explicit schemes, when the Courant number, which determines the accuracy and convergence of the solution, is less than 0.05, leads to a rapid accumulation of computational error and significantly degrades the accuracy of the numerical solution.

This limitation does not allow using the FDTD method for interpreting GPR data in environments with a sufficiently high conductivity or with its gradient change, which are regularly encountered in the natural environment. In this study, we use a scheme for the numerical integration of Maxwell's equations, in which there is no restriction on the integration step over time due to the influence of conductivity [Mingalev et al., 2019]. It is based on the explicit monotonic scheme of splitting by spatial directions and physical processes that allows us to use a significantly larger integration step in time than in the widely used FDTD method with the same calculation accuracy.

In this numerical modelling, our goal was to study the influence of the near-bottom layer with a gradient in electrical conductivity and permittivity on the receiving signal for further implication in GPR studies and data interpretation.

2   Numerical integration method

We use an explicit difference scheme for the numerical integration of Maxwell's equations on a regular spatial grid in Cartesian coordinates [Mingalev et al., 2019], which is as follows.

Let $r = (x, y, z)$ be the Cartesian coordinates; t – be the time; $E(r, t)$, $D(r, t)$, $H(r, t)$ and $B(r, t)$ be the electric and magnetic field strength and induction; $j(r, t)$ be the current density at t at a point with the radius vector r. Consider the Faraday and Maxwell equations in the SI system

$$\frac{\partial B}{\partial t} = -\text{rot}\, E(r, t)\,, \quad \frac{\partial D}{\partial t} = \text{rot}\, H(r, t) - j(r, t). \quad (1)$$

Let's supplement these equations with Ohm's law:

$$j(r, t) = \sigma(r) \cdot E(r, t), \quad (2)$$

where $\sigma(r)$ is the scalar conductivity of the medium, and with constitutive equations

$$D(r, t) = \varepsilon_0 \varepsilon(r) E(r, t)\,, \quad B(r, t) = \mu_0 \mu(r) H(r, t)\,, \quad (3)$$

where $\varepsilon(r)$ and $\mu(r)$ are dimensionless relative permittivity and permeability of the medium at a low

frequency limit; ε_0 and μ_0 are electric and magnetic permeability of vacuum. Let $c_0 = 1 / \sqrt{\varepsilon_0 \mu_0}$ be the velocity of light in vacuum; $c(r) = c_0 / \sqrt{\varepsilon(r) \mu(r)}$ be the velocity of light in medium at a point with the radius vector r. System (1)–(3) can be written as

$$\frac{\partial B}{\partial t} = -\text{rot}\, E\,, \quad \frac{\partial E}{\partial t} = \frac{c_0^2}{\varepsilon} \text{rot}\left(\frac{B}{\mu}\right) - \frac{\sigma}{\varepsilon_0 \varepsilon} E\,. \quad (4)$$

For the numerical integration of (4) we use the method of splitting by physical processes. The total integration step breaks down into two substeps. One of them is a substep of propagation, at which we the system of equations

$$\frac{\partial B}{\partial t} = -\text{rot}\, E\,, \quad \frac{\partial E}{\partial t} = \frac{c_0^2}{\varepsilon} \text{rot}\left(\frac{B}{\mu}\right)\,, \quad (5)$$

is integrated; the second step is a substep of signal attenuation, at which the system of equations

$$\frac{\partial E}{\partial t} = -\frac{\sigma}{\varepsilon_0 \varepsilon} E$$

is analytically integrated from formulas $E(r, t + \tau) = E(r, t) \exp\left(-\frac{\sigma(r)\tau}{\varepsilon_0 \varepsilon(r)}\right)$. The correct sequence of the substeps of splitting provides the second-order accuracy in time.

In the numerical integration of system (5), quite a lot of different schemes have been developed, including schemes of a higher order of accuracy, which are used for the equations of gas dynamics.

This scheme for integrating Maxwell's equations is fully applicable to the problem of simulating the propagation of a video pulse electromagnetic signal, as such as used in GROT 12 radars, in real environments and allows using a significantly larger time integration step than the widely used FDTD method with the same calculation accuracy.

In order to avoid the use of model absorbing layers, we use the following technique: the distance from the transmitter to the boundaries of the simulation area was chosen so that the signal reflected from the heterogeneity arrived at the receiving antenna much earlier than the signal reflected from the boundaries of the simulation area.

A video pulse with a given shape shown in Figure 1 is used as a probe pulse. This signal is conventionally divided into parts: the duration of the leading edge is T1; the front part duration is T2; the relaxation part duration is T3. The total duration T2 + T3 = T4 is up to 20 ns.

Figure 2 presents a model of a freshwater body with a near-bottom layer that has smooth (gradient) changes in the electrical parameters.

We have chosen the most common electrical parameters found in the natural environment for the model of the medium. It should be noted that the
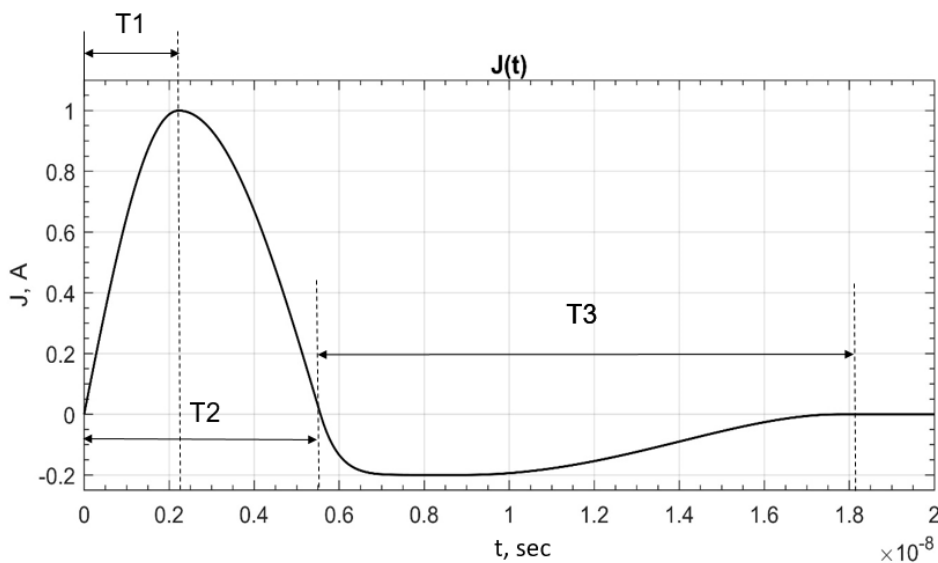
Figure 1: Dependence of the current in the antenna on time for a probing video pulse.
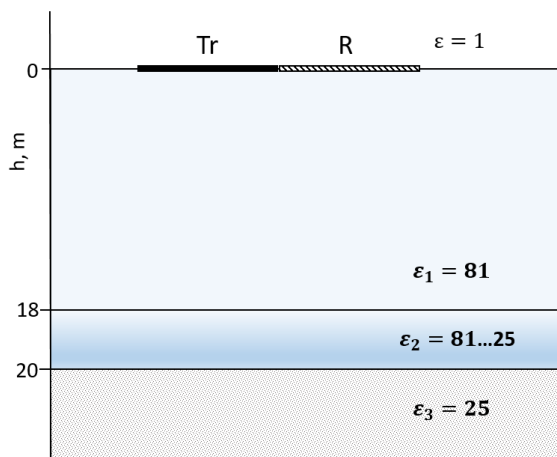

Figure 2: A model of a freshwater body with a near-bottom layer: Tr – transmitter, R – receiver.

Figure 3: The gradient of the permittivity in the near-bottom layer at the depths from 18 m to 19 m, 20 m and 22 m; $\sqrt{\varepsilon_2}$ decreases linearly from 9 to 5; $\sigma = 0.001$ S/m.

range of change in permittivity does not exceed an order of magnitude, while electrical conductivity can vary by several orders of magnitude. Moreover, the gradients of the permittivity and electrical conductivity at the bottom of freshwater bodies, as a rule, have opposite signs, because the permittivity is higher, and the conductivity of water is lower than that of the silt sediments.

3   RESULTS AND DISCUSSION

To study the influence of the permittivity gradient on the shape of the reflected signal, we use a model of the freshwater body with a gradient layer of different thicknesses: 1 m, 2 m, and 4 m, where $\sqrt{\varepsilon_2}$ decreases linearly from 9 to 5 (Figure 3).

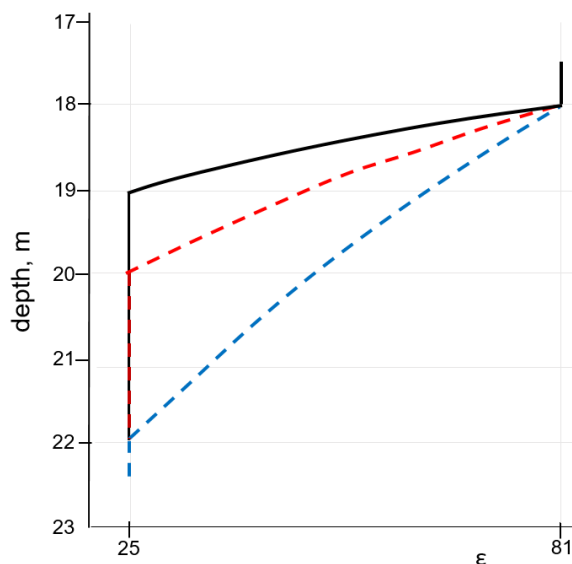The analysis of the calculations allows us to explain the effect sometimes observed in studies in

water bodies: the apparent decrease in the water depth according to GPR data when compared with direct measurements.

In Figure 4, it can be seen that with an increase in the thickness of the gradient layer, the discrepancy between the true water depth and the one calculated from time delays of the signal increases increases. Taking the permittivity value $\varepsilon = 81$, the time delay for a depth of 19 m is 1140 ns, for 20 m – 1200 ns, and for 22 m – 1320 ns. The extremum of the reflected signal noticeably deviates from the calculated values the stronger, the greater the depth of the gradient layer. The first arrival corresponds to the top of the gradient layer, the
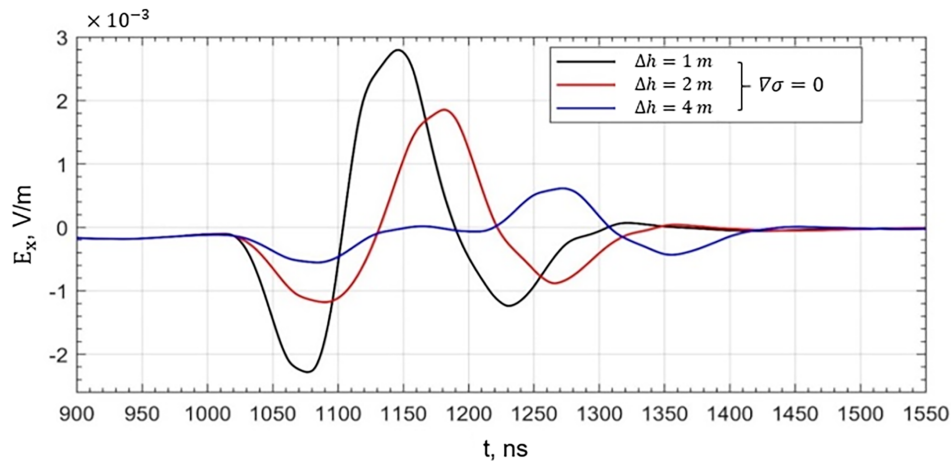
Figure 4: Calculated electric field strength of the reflected signal E_x for media with different thickness (Δh) of the layer with permittivity gradient.

second indicates the reflection from the bottom. For 2-meter gradient layer the difference between time delays assessed with the permittivity value $\varepsilon = 81$ and numerical modelling reaches 40 ns, and for 4-meter gradient layer – 70 ns. An error of 40 ns for $\varepsilon = 81$ corresponds to a depth error of 0.67 m.

Thus, with an increase in the thickness of the gradient near-bottom layer, the error in determining the water depth using $\varepsilon = 81$ increases, while the amplitude of the reflected signal decreases, which leads to a decrease, other things being equal, of the resolution. Besides, in real GPR data, it is necessary to take into account the accuracy of GPR measurements, which is also determined by the technical characteristics of the equipment, in particular, by the implemented registration technique, that provides further reduction in the depth resolution in case of frequency or time gating with frequency filtering and nonlinear amplification of amplitudes [*Gulevich et al.*, 2021].

To study the impact of the electrical conductivity gradient on the shape of the reflected signal, we consider the model of the medium shown in Figure 5, the permittivity is assumed to be constant.

Figure 6 shows the influence of the gradient of the electrical conductivity on the amplitude and shape of the reflected signal for the chosen models of the medium.

Comparison of the results shows that the electrical conductivity gradient in the water body affects the estimate of its water depth but less significantly compared to the influence of the permittivity gradient. Having an electrical conductivity gradient in the near-bottom layer, the two most intense extrema with almost equal amplitudes are observed: the first and the next one of opposite polarity (Figure 6). It is seen that the extrema of the reflected signals for the gradient of the permittivity and electrical conductivity have opposite polarity (Figure 4, Figure 6).
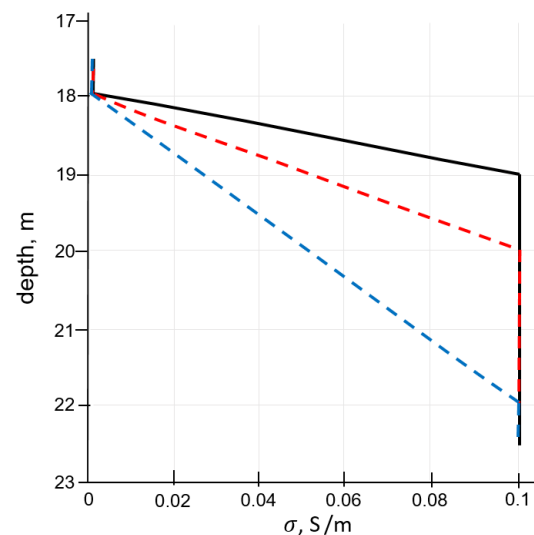

Figure 5: The gradient of the electrical conductivity in the near-bottom layer at the depths from 18 m to 19 m, 20 m and 22 m; σ linearly increases from 0.001 S/m to 0.1 S/m; $\varepsilon = 81$.

Moreover, as can be seen from the simulation results (Figure 4, Figure 6), in the presence of the near-bottom gradient layer, an additional first extremum appears in the amplitude of the reflected signal, which corresponds to the top of the gradient layer. The appearance of additional reflecting boundaries is typical for ground-penetrating radar surveys.

Based on the presented results of the numerical modelling, additional reflecting boundaries can be a sign of the inhomogeneity of the bottom water layer in terms of permittivity and conductivity.

Changing the thickness of the gradient layer (Figure 3, Figure 5). has an impact on the amplitude values of reflected signals but the pattern of the evolution of the amplitudes remains (Figure 4, Figure 6).
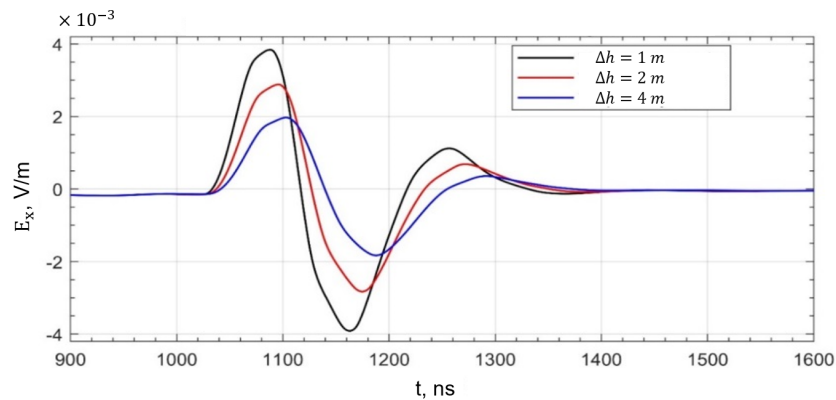
Figure 6: Calculated electric field strength of the reflected signal E_x for media with different thickness (Δh) of the layer with electrical conductivity gradient.
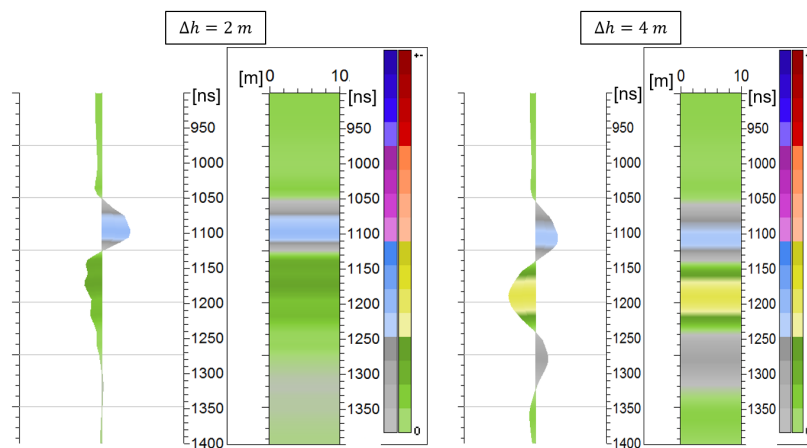

Figure 7: Synthetic waveforms (A-scans) and radargrams (B-scans) for a freshwater model with a near-bottom gradient layer of the thickness 2 m (left) and 4 m (right). $\sqrt{\varepsilon_2}$ decreases linearly from 9 to 5; σ increases linearly from 0.001 S/m to 0.1 S/m.

Figure 7 shows synthetic waveforms and radargrams for a model with a gradient layer with a thickness of 2 and 4 m, taking into account the gradient change in both permittivity and electrical conductivity in the usual representation for GPR. The pattern of the permittivity gradient is shown in Figure 3 with the red dotted line and of the electrical conductivity gradient – in Figure 5 with a red dotted line.

It can be seen that with an increase in the thickness of the gradient layer more additional reflective boundaries appear on the radargram (Figure 7).

The total effect of the gradient of electrical parameters in the near-bottom layer strongly depends on the ratio of the actual values of electrical conductivity and permittivity. Accordingly, the accuracy of the water depth estimate is also determined by the spatial distribution of electrical parameters in the water body.

The calculated evolution of the video pulse signal shows that the gradient layer can significantly reduce the depth resolution, complicate interpretation and affect the survey accuracy, that is, mask useful information in real GPR studies.

It should be noted that the radio pulse signal, which initially contains more amplitude extrema than the aperiodic signal, the shape of which was taken for calculations (Figure 1), is characterized by the appearance of a number of parasitic boundaries on the ground-penetrating radar data, i.e. "ringing".

4 CONCLUSIONS

The accuracy of determining water depth in a freshwater body depends on a pattern of electric conductivity and permittivity distribution in the near-bottom layer, which is heterogeneous in natural environments.

Additional reflective boundaries on radargrams in the bottom layer may indicate gradient changes in electrical properties in the water body. These multiple boundaries can mask the reflection from the bottom of a water body and complicate the interpretation of GPR data.

In real GPR surveys, it is necessary to take into account the accuracy of GPR measurements, also determined by the technical characteristics of the equipment, in particular, by the implemented registration technique, which can further reduce the depth resolution.

Conflict of interest

All authors declare no conflicts of interest in this paper.

REFERENCES

Archer, D. G., and P. Wang, The Dielectric Constant of Water and Debye-Hückel Limiting Law Slopes, *Journal of Physical and Chemical Reference Data*, *19*(2), 371–411, doi:10.1063/1.555853, 1990.

Bobrov, N. Y., V. V. Dmitriev, S. S. Krylov, T. V. Parshina, G. V. Pryahina, and I. V. Fedorova, On the possibility of georadiolocation application for hydrological investigations in the river mouth areas, *Vestnik of SPbSU. Series7. Geography and Geology*, *7*(2), 76–81, (In Russian), 2008.

Bristow, C. S., and H. M. Jol, An introduction to ground penetrating radar (GPR) in sediments, *Geological Society, London, Special Publications*, *211*(1), 1–7, doi:10.1144/gsl.sp.2001.211.01.01, 2003.

Catenaccio, A., Y. Daruich, and C. Magallanes, Temperature dependence of the permittivity of water, *Chemical Physics Letters*, *367*(5-6), 669–671, doi:10.1016/S0009-2614(02)01735-9, 2003.

Giannopoulos, A., Modelling ground penetrating radar by GprMax, *Construction and Building Materials*, *19*(10), 755–762, doi:10.1016/j.conbuildmat.2005.06.007, 2005.

Gulevich, O. A., About scanning depth in georadiolocation considering the phenomenon of interference, *Journal of Radio Electronics*, *2020*(9), doi:10.30898/1684-1719.2020.9.8, (In Russian), 2020.

Gulevich, O. A., L. B. Volkomirskaya, A. E. Reznikov, and V. V. Varenkov, Typical effects of the registration technology implemented in the GPR receiver, in *NSG2021 Conference Proceedings, 27th European Meeting of Environmental and Engineering Geophysics, Aug 2021*, pp. 1–5, Vol. 2021, doi:10.3997/2214-4609.202120153, 2021.

Jol, H. M., and D. G. Smith, Ground penetrating radar of northern lacustrine deltas, *Canadian Journal of Earth Sciences*, *28*(12), 1939–1947, doi:10.1139/e91-175, 1991.

Kane, S. Y., Numerical solution of initial boundary value problems involving maxwell's equations in isotropic media, *IEEE Transactions on Antennas and Propagation*, *14*(3), 302–307, doi:10.1109/TAP.1966.1138, 1966.

Mingalev, I. V., O. V. Mingalev, O. I. Akhmetov, and Z. V. Suvorova, Explicit Splitting Scheme for Maxwell's Equations, *Mathematical Models and Computer Simulations*, *11*, 551–563, doi:10.1134/S2070048219040094, 2019.

Owen, B. B., R. C. Miller, C. E. Milner, and H. L. Cogan, The Dielectric Constant Of Water As A Function Of Temperature And Pressure, *The Journal of Physical Chemistry*, *65*(11), 2065–2070, doi:10.1021/j100828a035, 1961.

Paul, D. L., and C. J. Railton, Spherical ADI FDTD method with application to propagation in the Earth ionosphere cavity, *IEEE Transactions on Antennas and Propagation*, *60*(1), 310–317, doi:10.1109/TAP.2011.2167940, 2012.

Schwarzburg, A. B., Video pulses and non-periodic waves in dispersing media (exactly solvable models), *Uspekhi Fizicheskikh Nauk*, *168*(1), 85–103, doi:10.30898/1684-1719.2021.11.8, (In Russian), 1998.

Simpson, J. J., Current and future applications of 3-D global Earth-ionospheric models based on the full-vector Maxwell's equations FDTD method, *Surveys in Geophysics*, *30*(2), 105–130, doi:10.1007/s10712-009-9063-5, 2009.

Simpson, J. J., and A. Taflove, A review of progress in FDTD Maxwell's equations modeling of impulsive subionospheric propagation below 300 kHz, *IEEE Transactions on Antennas and Propagation*, *55*(6), 1582–1590, doi:10.1109/TAP.2007.897138, 2007.

Smith, D. G., and H. M. Jol, Ground-penetrating radar investigation of a Lake Bonneville deita, Provo level, Brigham City, Utah, *Geology*, *20*(12), 1083-1086, doi:10.1130/0091-7613(1992)020<1083:GPRIOA>2.3.CO;2, 1992.

Somaraju, R., and J. Trumpf, Frequency, Temperature and Salinity Variation of the Permittivity of Seawater, *IEEE Transactions on Antennas and Propagation*, *54*(11), 3441–3448, doi:10.1109/TAP.2006.884290, 2006.

Warren, C., A. Giannopoulos, and I. Giannakis, gprMax: Open source software to simulate electromagnetic wave propagation for Ground Penetrating Radar, *Computer Physics Communications*, *209*, 163–170, doi:10.1016/j.cpc.2016.08.020, 2016.

Yu, Y., and J. J. Simpson, An E-J collocated 3-D FDTD model of electromagnetic wave propagation in magnetized cold plasma, *IEEE Transactions on Antennas and Propagation*, *58*(2), 469–478, doi:10.1109/TAP.2009.2037706, 2010.